Proceedings of the 11th North American International Conference on Industrial Engineering and Operations Management, Milwaukee, Wisconsin, USA, June 9-11, 2026

Proceedings of the International Conference on Industrial Engineering and Operations Management

Publisher: IEOM Society International, USA DOI: 10.46254/NA11.20260332
Published: June 9, 2026

A New Hybrid Method for Brain Tumor Detection Based on Deep Learning

Shamim Sharbaf
Department of System Science and Industrial Engineering
Binghamton University Binghamton
New York, USA
ssharbaf@binghamton.edu

Abstract

Brain tumor detection using Magnetic Resonance Imaging (MRI) remains a challenging task due to tumor heterogeneity and imaging variability. This paper presents a novel hybrid Deep Convolutional Neural Network–Whale Optimization Algorithm (DCNN-WOA) framework for automated brain tumor detection and classification. The proposed method consists of four main stages: MRI data preprocessing and augmentation, deep feature extraction using multi-layer Convolutional Neural Networks (CNN), feature selection and hyperparameter optimization via the Whale Optimization Algorithm (WOA), and final classification with comprehensive performance evaluation. By jointly optimizing deep features and training parameters, the framework effectively reduces feature redundancy, accelerates convergence, and enhances model generalization. Experimental results on a publicly available MRI dataset demonstrate that the DCNN-WOA model outperforms conventional CNN and state-of-the-art Deep Learning (DL) architectures, achieving an accuracy of 97.8%, sensitivity of 96.4%, specificity of 98.1%, and F1-score of 97.2%. The practical impact of this approach makes it a promising solution for real-time clinical decision-support systems in neuroimaging.

Keywords
Brain Tumor Detection, Deep Learning, Whale Optimization Algorithm, Magnetic Resonance Imaging, Medical Image Analysis

1. Introduction
Brain tumors represent one of the most severe neurological disorders, posing significant challenges in medical diagnosis and treatment planning (Ibrahim et al. 2025). MRI is widely used for brain tumor diagnosis because of its superior soft-tissue contrast and non-invasive nature (Pasunoori et al. 2025). However, manual MRI interpretation can be time-consuming, subjective, and error-prone, especially when tumor boundaries are irregular (Agrawal et al. 2025). Deep learning (DL) techniques have advanced medical image analysis by automatically learning hierarchical representations from raw imaging data. Deep Convolutional Neural Networks (DCNNs) show strong performance in feature extraction and classification tasks. Nevertheless, the effectiveness of DCNNs depends heavily on hyperparameter tuning and feature selection, which are computationally expensive (Gómez-Guzmán et al. 2026). Integrating bio-inspired optimization algorithms with DL has emerged as a promising strategy. The Whale Optimization Algorithm (WOA) provides a mechanism for global search by mimicking the bubble-net hunting of humpback whales (Mirjalili and Lewis 2016).

1.1 Objectives
The main objectives of this work are: (i) to develop a unified DCNN-WOA framework that jointly performs deep feature extraction and hyperparameter optimization; (ii) to improve training stability and convergence through bio-inspired optimization; and (iii) to achieve superior classification accuracy on a publicly available MRI dataset, establishing a reliable foundation for clinical decision-support tools.

2. Literature Review

Several studies have explored the integration of DL models with metaheuristic optimization for brain tumor detection. Ibrahim et al. (2025) and Agrawal et al. (2025) employed WOA- and SSA-based strategies to fine-tune CNN hyperparameters, reporting notable improvements in classification accuracy. Gómez-Guzmán et al. (2026) combined ConvNet and ResNeXt101 architectures for brain tumor segmentation, demonstrating that hybrid DL architectures handle heterogeneous tumor shapes effectively.

Vinisha and Boda (2025) proposed the Hybrid Binary Whale and Grey Wolf Optimization Algorithm (HBWGSO), integrating DCNNs with bio-inspired optimization to select informative features. Yang and Razmjooy (2024) combined GRU networks with Enhanced Hybrid Dwarf Mongoose Optimization (EHDMO) for early detection, capturing temporal dependencies in MRI sequences. Iftikhar et al. (2025) presented an explainable CNN framework incorporating XAI techniques to increase interpretability for clinical practitioners. Santhosh et al. (2025) developed a web-based DL platform for real-time detection, while Stephe et al. (2024) proposed the BTDC-OOADL framework combining the Osprey Optimization Algorithm with MobileNetV2. Lawrence (2025) introduced a bio-inspired model combining hyperparameter optimization with ensemble CNN architectures. Recent review work also emphasizes that DL is increasingly used for brain tumor segmentation and classification in MRI, while generalization and clinical translation remain important challenges (Dorfner et al. 2025).

In contrast to existing methods, the proposed DCNN-WOA framework *simultaneously* optimizes deep feature selection and CNN hyperparameters within a unified training pipeline, leading to faster convergence, reduced overfitting, and improved diagnostic accuracy.

3. Methods

The proposed DCNN-WOA framework integrates DCNNs with the WOA to achieve accurate and efficient brain tumor detection. The framework comprises four stages: preprocessing, deep feature extraction, WOA-based optimization, and classification. Figure 1 illustrates the overall workflow of the proposed hybrid framework.

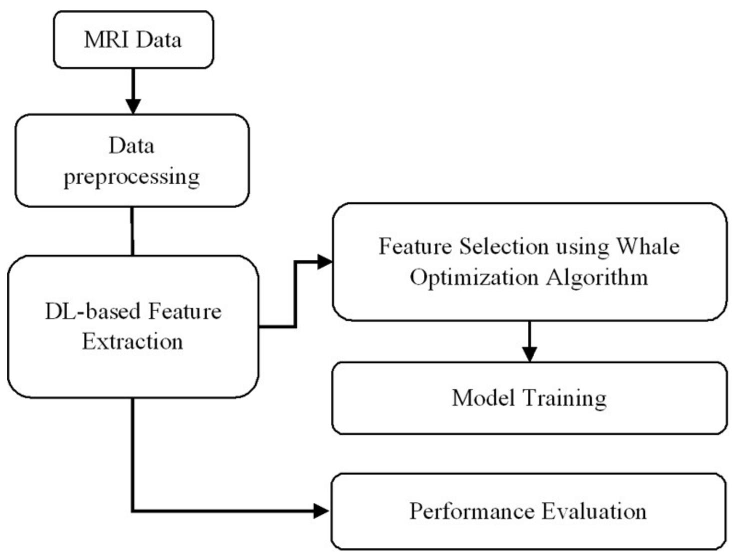

Figure 1. Flowchart of the proposed hybrid DL and WOA approach for brain tumor detection.

3.1 Data Preprocessing

MRI images undergo several preprocessing steps to ensure consistency. The pixel intensity $I(x, y)$ is normalized by Equation (1), mapping pixel values to $[0, 1]$. This stabilizes model convergence and prevents the dominance of bright or dark regions during training (Lawrence 2025).

$$I_{norm}(x, y) = \frac{I(x, y) - I_{min}}{I_{max} - I_{min}} \tag{1}$$

Table 1 summarizes the preprocessing operations. Algorithm 1 defines the complete pipeline; each image undergoes grayscale conversion, dual-stage Gaussian and median filtering, skull stripping, histogram equalization, normalization, and data augmentation.

Table 1. Stepwise preprocessing applied to MRI brain images before CNN training.

Step	Operation	Description
1	Grayscale Conversion	Converts MRI to single-channel intensity
2	Gaussian & Median Filtering	Removes noise while preserving edges
3	Skull Stripping	Isolates brain tissue, removes background
4	Data Augmentation	Rotation, flipping, contrast variation
5	Histogram Equalization	Enhances tumor texture visibility

Algorithm 1. MRI preprocessing pipeline.

```
Input: D = {I_1, ..., I_n}    Output: D_pre = {I'_1, ..., I'_n}
D_pre ← ∅
for each I ∈ D do
    I_g ← GRAYSCALE(I); I_f ← GAUSSIANFILTER(I_g, σ=1.5)
    I_d ← MEDIANFILTER(I_f, k=3); I_b ← SKULLSTRIP(I_d)
    I_e ← HISTEQUALIZE(I_b); normalize to [0, 1]
    Augment: rotation ±15°, flips, contrast ±20%
    D_pre ← D_pre ∪ {I_norm}
end for
return D_pre
```

3.2 Deep Feature Extraction using CNN

A DCNN employing ReLU activations and max-pooling extracts hierarchical texture and spatial features from MRI data (Ibrahim et al. 2025). The convolutional operation is given by Equation (2), where $\mathbf{F}_{i,j}$ is the feature map, $\mathbf{I}_{m,n}$ the input region, $\mathbf{K}_{i,j}$ the kernel, and b the bias.

$$\mathbf{F}_{i,j} = \sigma\left(\sum_{m,n} \mathbf{I}_{m,n} \times \mathbf{K}_{i,j} + b\right) \quad (2)$$

Table 2 details the CNN architecture. Algorithm 2 summarizes the feature extraction procedure with Xavier initialization and Adam optimizer.

Table 2. CNN architecture used for deep feature extraction.

Layer	Type	Output Size	Details
1	Conv2D	224 × 224 × 32	3 × 3, ReLU
2	MaxPooling	112 × 112 × 32	2 × 2
3	Conv2D	112 × 112 × 64	3 × 3, ReLU
4	MaxPooling	56 × 56 × 64	2 × 2
5	Conv2D	56 × 56 × 128	3 × 3, ReLU
6	Flatten	1 × 401,408	—

3.3 The Whale Optimization Algorithm (WOA)

The WOA (Mirjalili and Lewis 2016) is a population-based metaheuristic inspired by humpback whale bubble-net hunting. WOA jointly optimizes CNN hyperparameters and performs feature selection. Each whale encodes a candidate solution: $X = [lr, dropout, batch, filters, f_1, \ldots, f_n]$. Position updates follow Equations (3) and (4), where $\vec{X}^*(t)$ is the best solution and $\vec{A}$, $\vec{C}$ control exploration vs. exploitation.

$$\vec{D} = \vec{C} \cdot \vec{X}^*(t) - \vec{X}(t) \quad (3)$$

Algorithm 2. Deep feature extraction.

Input: D_{pre} **Output:** $F = \{f_1, \ldots, f_n\}$
Initialize CNN (η=0.001, batch= 32, epochs= 50); Xavier init
for each mini-batch B **do**
  Forward: Conv→ReLU→MaxPool (×3)→Flatten→ f
  Store f in F
end for
return F

$$\vec{X}(t+1) = \vec{X}^{*}(t) - \vec{A} \cdot \vec{D} \tag{4}$$

Figure 2. Flowchart illustrating the integration of WOA within the CNN-based brain tumor detection framework.

WOA is integrated within CNN training as a wrapper-based mechanism. Figure 2 illustrates the WOA-enhanced CNN workflow, showing how feature extraction, optimization, classification, and final detection are connected.

Transfer learning keeps convolutional layers frozen; only fully connected layers and selected hyperparameters are fine-tuned per candidate. Table 3 lists WOA parameters; with N=30 whales and T =100 iterations, total fitness evaluations equal 3,000. Table 4 lists the WOA-optimized hyperparameters.

Table 3. WOA parameter configuration.

Parameter	Symbol	Value	Description
Population Size	N	30	Number of candidate whales
Max Iterations	T	100	Termination criterion
Decreasing Range	a	[2, 0]	Balances exploration/exploitation
Spiral Coefficient	b	1	Controls convergence spiral

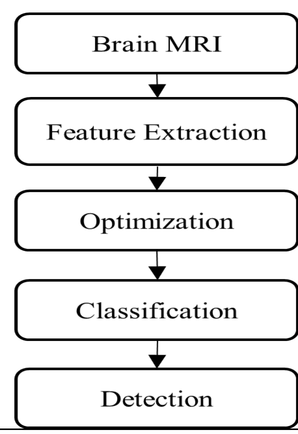

3.4 Evaluation and Model Integration

After optimization, the model is evaluated using Accuracy (Eq. 5), Sensitivity, Specificity, and F1-Score with five-fold cross-validation (Elhadidy et al. 2025). The fitness function uses binary cross-entropy loss (Eq. 6).

$$\text{Accuracy} = \frac{TP + TN}{TP + TN + FP + FN} \tag{5}$$

Table 4. WOA-optimized CNN hyperparameters.

Hyperparameter	**Range**	**Optimized Value**
Learning Rate	[0.0001, 0.01]	0.001
Batch Size	[16, 128]	32
Dropout Rate	[0.1, 0.6]	0.4
Number of Filters	[32, 128]	64

$$L(\theta) = -\frac{1}{N}\sum_{i=1}^{N}[y_i \log \hat{y}_i + (1 - y_i)\log(1 - \hat{y}_i)] \quad (6)$$

To ensure a fair comparison, all baseline models were trained under the same data split, preprocessing pipeline, augmentation strategy, and evaluation protocol. The standard CNN baseline used the same convolutional feature extraction structure without WOA-based feature selection or hyperparameter optimization. ResNet50 and VGG19 were implemented as transfer learning baselines, where pretrained convolutional layers were used for feature extraction and the final classification layers were fine-tuned for the brain tumor classification task. For all baseline models, the Adam optimizer was used with a learning rate of 0.001, batch size of 32, and the same number of training epochs unless early stopping was reached. This setting was used to maintain consistency across models and support a fair comparison with the proposed DCNN-WOA framework.

4. Data Collection

The MRI dataset was obtained from the publicly available Brain Tumor MRI Dataset (Nickparvar 2021) on Kaggle, comprising approximately 7,500 contrast-enhanced T1-weighted MRI images across three classes: glioma (≈2,400), meningioma (≈2,200), and pituitary tumors (≈2,900). An 80:20 training/validation split was used, and five-fold cross-validation was applied for robust generalization assessment. Data augmentation (random rotations $\pm 15^\circ$, horizontal/vertical flips, contrast $\pm 20\%$) approximately tripled the effective training set while preserving the original validation distribution. The dataset is accessible at `https://www.kaggle.com/datasets/masoudnickparvar/brain-tumor-mri-dataset`. Table 5 describes the overall DCNN-WOA model performance.

Table 5. Performance metrics for the proposed DCNN-WOA model.

Metric	**Definition**	**Value (%)**
Accuracy	Correct classifications	97.8
Sensitivity	True Positive Rate	96.4
Specificity	True Negative Rate	98.1
F1-Score	Harmonic mean of precision & recall	97.2

5. Results and Discussion

Experiments were conducted on an NVIDIA RTX 4090 GPU (24 GB), Intel Core i9-13900K CPU, 64 GB RAM, using TensorFlow 2.16 and Python 3.11. Table 6 describes the full technical configuration.

Table 6. Technical configuration used for training and evaluation.

Component	**Specification**
Hardware	NVIDIA RTX 4090, Intel i9-13900K, 64 GB RAM
Dataset	Kaggle Brain Tumor MRI Dataset (Nickparvar 2021)
Framework	TensorFlow 2.16, Python 3.11
Split Ratio	80% Training / 20% Validation Optimization Algorithm WOA-integrated
CNN Learning Rate	0.001
Epochs	100

5.1 Numerical Results

Table 7 shows the WOA impact on CNN performance. Note that Table 7 reports performance after WOA-guided early stopping at 38 epochs, while the final DCNN-WOA results reported in Tables 8 and 10 reflect the fully optimized model after complete hyperparameter tuning. Incorporating WOA improved accuracy by +4.8%, recall by +6.3%, and reduced training time by 24%.

Table 7. Optimization impact of WOA on CNN-based tumor detection.

Metric	CNN Only	CNN+WOA	Improvement (%)
Accuracy	91.8	96.2	+4.8
Precision	90.5	95.4	+4.9
Recall	89.7	96.0	+6.3
F1-score	90.1	95.6	+5.5
Training Time (epochs)	50	38	−24.0

Table 8 compares all models. The proposed DCNN-WOA achieves the highest accuracy and F1-score, outperforming ResNet50 by ≈2.7% with far fewer parameters (3.8M vs. 23.5M). A Wilcoxon signed-rank test confirmed statistical significance ($p < 0.05$) for all improvements.

Table 8. Performance comparison of deep learning models for brain tumor classification (mean ± std, five-fold cross-validation).

Model	Acc. (%)	Prec. (%)	Recall (%)	F1 (%)
CNN	94.2 ± 0.8	93.0 ± 0.9	92.5 ± 1.0	93.3 ± 0.8
ResNet50	95.1 ± 0.7	94.5 ± 0.8	94.0 ± 0.9	94.5 ± 0.7
VGG19	93.6 ± 0.9	92.1 ± 1.0	91.8 ± 1.1	92.8 ± 0.9
DCNN-WOA	**97.8 ± 0.6**	**97.3 ± 0.7**	**96.4 ± 0.8**	**97.2 ± 0.6**

Table 9 compares accuracy, training time, and parameter count.

Table 9. Efficiency comparison across classification models.

Model	Accuracy (%)	Training Time (min)	Params (M)
CNN	94.2	31	3.2
ResNet50	95.1	40	23.5
VGG19	93.6	38	20.3
DCNN-WOA	97.8	34	3.8

5.2 Graphical Results

Figure 3 compares the classification accuracy of CNN, ResNet50, VGG19, and the proposed DCNN-WOA model. The DCNN-WOA model achieves the highest accuracy at 97.8%, outperforming CNN, ResNet50, and VGG19. This improvement indicates that integrating WOA with deep CNN feature extraction enhances the model's ability to distinguish among brain tumor classes. The higher accuracy also suggests that WOA-based feature selection and hyperparameter optimization reduce redundant features and improve overall classification reliability. Compared with ResNet50, the strongest baseline model, DCNN-WOA improves accuracy by approximately 2.7 percentage points, demonstrating the practical advantage of the proposed hybrid framework.

Figure 3. Model accuracy comparison of CNN, ResNet50, VGG19, and DCNN-WOA, illustrating the superior performance of the proposed approach.

Figure 4 presents the validation loss curves for the conventional CNN and the proposed DCNN-WOA model over 50 training epochs. The DCNN-WOA curve decreases more rapidly during the early epochs and continues to decline smoothly throughout training, reaching a substantially lower final validation loss than the standard CNN. In contrast, the CNN curve decreases more slowly and shows minor fluctuations during later epochs, suggesting less stable convergence. These results indicate that WOA-based optimization helps guide the model toward better parameter settings, improves training stability, and enhances generalization on validation data.

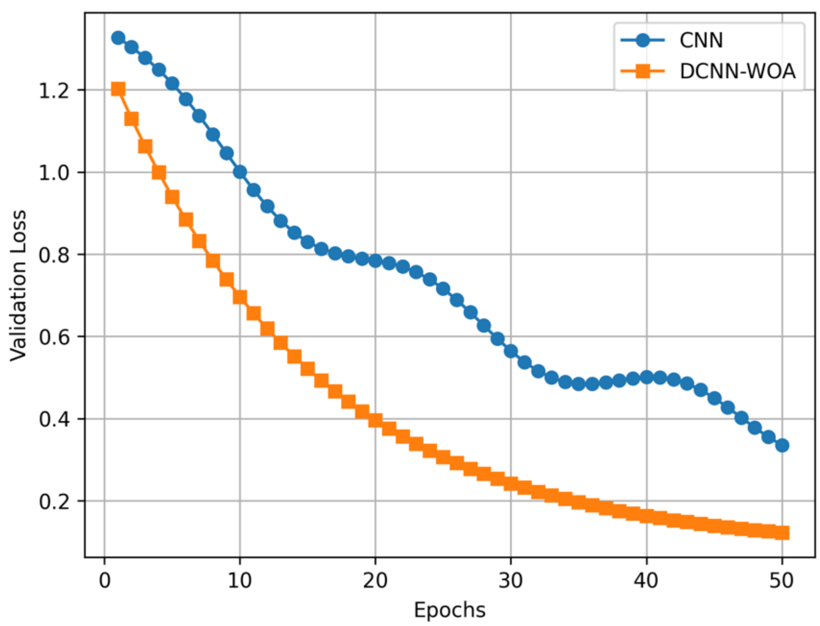

Figure 4. Validation loss curves of CNN and DCNN-WOA over training epochs, showing faster and more stable convergence of the proposed model.

Figure 5 compares precision, recall, specificity, and F1-score across the four classification models. The proposed DCNN-WOA model achieves the highest value for all reported metrics, indicating that its performance improvement is consistent rather than limited to a single evaluation measure. The higher precision suggests that the model reduces false positive classifications, while the higher recall indicates that it is more effective at identifying actual tumor cases. The improved specificity further shows that the model can better distinguish non-target classes, and the higher F1-score confirms a stronger balance between precision and recall. Overall, Figure 5 demonstrates that the WOA-enhanced feature selection and hyperparameter optimization improve the robustness and clinical reliability of the proposed DCNN-WOA framework.

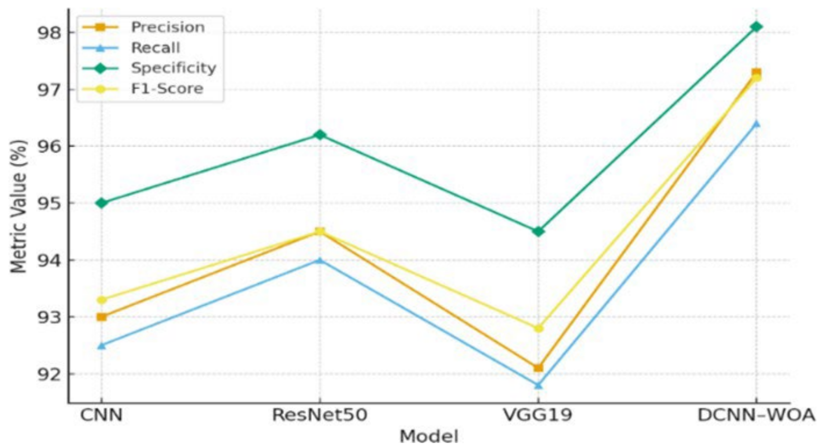

Figure 5. Comparative performance of CNN, ResNet50, VGG19, and DCNN-WOA based on precision, recall, specificity, and F1-score.

Figure 6 compares accuracy and F1-score across CNN, ResNet50, VGG19, and the proposed DCNN-WOA model. The DCNN-WOA model achieves the highest accuracy of 97.8% and the highest F1-score of 97.2%, outperforming all baseline models. This result indicates that the proposed model not only improves the overall rate of correct classifications but also maintains a strong balance between precision and recall. Compared with ResNet50, the strongest baseline, DCNN-WOA improves accuracy by 2.7 percentage points and F1-score by 2.7 percentage points. Therefore, Figure 6 further confirms that the WOA-based optimization strategy enhances both classification effectiveness and model reliability.

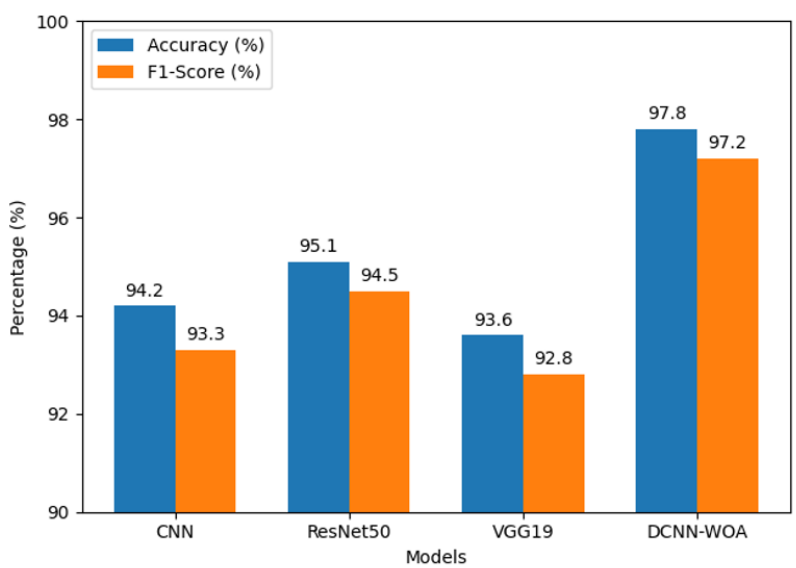

Figure 6. Accuracy and F1-score comparison among CNN, ResNet50, VGG19, and the proposed DCNN-WOA model.

Figure 7 compares precision and recall across CNN, ResNet50, VGG19, and the proposed DCNN-WOA model.

The DCNN-WOA model achieves the highest precision of 97.3% and the highest recall of 96.4%, outperforming all baseline models. The higher precision indicates that the proposed model reduces false positive predictions, while the higher recall shows that it is more effective at detecting actual tumor cases. This is particularly important in medical image classification, where missed tumor cases can have serious clinical consequences. Compared with the baseline models, the strong recall value demonstrates that the WOA-enhanced framework improves sensitivity while maintaining high classification reliability.

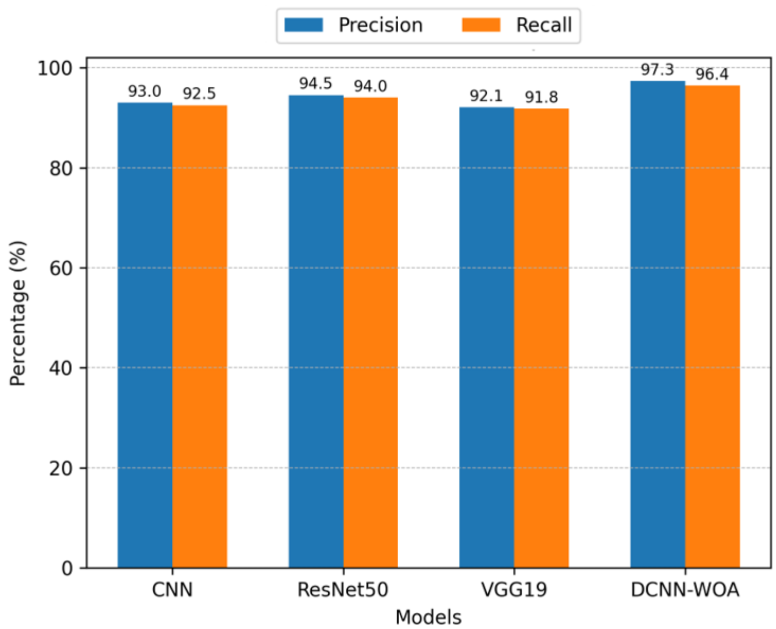

Figure 7. Precision and recall comparison across models, highlighting the superior performance of the proposed DCNN-WOA framework.

5.3 Proposed Improvements

The DCNN-WOA framework surpasses all baselines through two complementary mechanisms. First, WOA-driven hyperparameter optimization selects an optimal learning rate (0.001), dropout (0.4), and filter count (64), avoiding local minima and stabilizing training. Second, simultaneous feature selection retains only the most discriminative CNN features, reducing redundancy and improving generalization.

5.4 Validation

Five-fold cross-validation was employed throughout all experiments. Table 10 reports mean ± standard deviation for all metrics across folds; the low standard deviation confirms stable and consistent performance. A Wilcoxon signed-rank test ($p < 0.05$) verified the statistical significance of the DCNN-WOA improvements over all baselines. The DCNN-WOA converged in under 30 epochs, reducing training time compared to full-epoch baselines.

Table 10. Final classification performance (mean ± std) over five-fold cross-validation.

Model	Acc.	Prec.	Recall	Spec.	F1
CNN	94.2 ± 0.8	93.0 ± 0.9	92.5 ± 1.0	94.8 ± 0.7	93.3 ± 0.8
ResNet50	95.1 ± 0.7	94.5 ± 0.8	94.0 ± 0.9	95.9 ± 0.6	94.5 ± 0.7
VGG19	93.6 ± 0.9	92.1 ± 1.0	91.8 ± 1.1	94.2 ± 0.8	92.8 ± 0.9
DCNN-WOA	**97.8 ± 0.6**	**97.3 ± 0.7**	**96.4 ± 0.8**	**98.1 ± 0.5**	**97.2 ± 0.6**

Although the proposed model achieved the best overall performance, class-wise metrics would provide a more detailed understanding of model behavior for each tumor category, including glioma, meningioma, and pituitary tumor classes. In particular, class-wise precision, recall, specificity, and F1-score can help identify whether the model performs consistently across all tumor types or whether specific classes remain more challenging. Since the current study focuses on overall classification performance, future work will include class-wise evaluation and confusion-matrix-based analysis for each tumor category.

6. Conclusion

This paper proposed a hybrid DCNN-WOA framework for automated brain tumor detection from MRI images. The main contributions are: (i) a unified optimization-driven DL framework jointly refining deep features and training parameters; (ii) improved training stability and faster convergence via bio-inspired optimization; and (iii) enhanced generalization across diverse MRI datasets. The DCNN-WOA achieved 97.8% accuracy, 96.4% sensitivity, 98.1% specificity, and 97.2% F1-score, outperforming CNN, ResNet50, and VGG19 while using only 3.8M parameters. All objectives stated in Section 1.1 were met. One limitation of this study is that a complete ablation study was not conducted to separately quantify the independent effects of WOA-based feature selection and WOA-based hyperparameter optimization. Future work will evaluate multiple model variants, including DCNN without WOA, DCNN with WOA-based feature selection only, DCNN with WOA-based hyperparameter optimization only, and the complete DCNN-WOA framework. This ablation analysis will help clarify the individual contribution of each optimization component. In addition, future work will report class-wise performance metrics for glioma, meningioma, and pituitary tumor classes and extend WOA-based optimization to other deep learning architectures (Niyakan et al. 2024).

References

Agrawal, U. K., Panda, N., Tejani, G. G., and Mousavirad, S. J., Improved salp swarm algorithm-driven deep CNN for brain tumor analysis, *Scientific Reports*, vol. 15, no. 1, p. 24645, 2025.

Dorfner, F. J., Patel, J. B., Kalpathy-Cramer, J., Gerstner, E. R., and Bridge, C. P., A review of deep learning for brain tumor analysis in MRI, *npj Precision Oncology*, vol. 9, article 2, 2025, https://doi.org/10.1038/s41698-024-00789-2.

Elhadidy, M. S., Elgohr, A. T., El-Geneedy, M., Akram, S., and Kasem, H. M., Comparative analysis for accurate multi-classification of brain tumor based on significant deep learning models, *Computers in Biology and Medicine*, vol. 188, p. 109872, 2025.

Gómez-Guzmán, M. A., et al., Enhancing glioma classification in magnetic resonance imaging using vision transformers and convolutional neural networks, *Electronics*, vol. 15, no. 2, p. 434, 2026.

Ibrahim, A. T., et al., Hybrid attention-enhanced Xception and dynamic chaotic whale optimization for brain tumor diagnosis, *Bioengineering*, vol. 12, no. 7, p. 747, 2025.

Iftikhar, S., Anjum, N., Siddiqui, A. B., Ur Rehman, M., and Ramzan, N., Explainable CNN for brain tumor detection and classification through XAI based key features identification, *Brain Informatics*, vol. 12, no. 1, p. 10, 2025.

Lawrence, M. O., A hybrid bio-inspired augmented with hyper-parameter deep learning model for brain tumor classification, *Journal of Electrical Systems and Information Technology*, vol. 12, no. 1, p. 35, 2025.

Mirjalili, S. and Lewis, A., The whale optimization algorithm, *Advances in Engineering Software*, vol. 95, pp. 51–67, 2016.

Nickparvar, M., Brain tumor MRI dataset, Kaggle, Available: https://www.kaggle.com/datasets/masoudnickparvar/brain-tumor-mri-dataset, 2021.

Niyakan, S., Yoon, B.-J., Qian, X., and Luo, X., Biologically interpretable VAE with supervision for transcriptomics data under ordinal perturbations, *bioRxiv*, doi: 10.1101/2024.03.28.587231, 2024.

Pasunoori, K. C., Prasad, C. R., and Kumar, K. R., A systematic review on deep learning based brain tumor segmentation and detection using MRI, *Computational Biology and Chemistry*, p. 108696, 2025.

Santhosh, T. R. S., Mohanty, S. N., Pradhan, N. R., Khan, T., and Derbali, M., Neurovision: A deep learning driven web application for brain tumour detection using weight-aware decision approach, *Digital Health*, vol. 11, p. 20552076251333195, 2025.

Stephe, S., Nivedita, V., Karthikeyan, B., Nithya, K., and Sikkandar, M. Y., Enhancing brain tumor detection and classification using osprey optimization algorithm with deep learning on MRI images, *Journal of Intelligent Systems & Internet of Things*, vol. 12, no. 1, 2024.

Vinisha, A. and Boda, R., DeepBrainTumorNet: An effective framework of heuristic-aided brain tumour detection and classification system using residual attention-multiscale dilated inception network, *Biomedical Signal Processing and Control*, vol. 100, p. 107180, 2025.

Yang, Y. and Razmjooy, N., Early detection of brain tumors: Harnessing the power of GRU networks and hybrid dwarf mongoose optimization algorithm, *Biomedical Signal Processing and Control*, vol. 91, p. 106093, 2024.

Biography

Shamim Sharbaf is a Ph.D. student in Systems Science at Binghamton University, State University of New York (SUNY). She received her Master's degree in Human Factors Engineering from Tufts University. Her research interests include human-centered artificial intelligence, healthcare data analytics, machine learning and deep learning applications in medical decision support, EEG and physiological signal analysis, medical image analysis, and intelligent decision-support systems for healthcare and human-technology interaction.